Design Optimization of a Surface Micromachined Electro-Thermal Beam Flexure Polysilicon Actuator

Amarendra Atre

The George W Woodruff School of Mechanical Engineering
Georgia Institute of Technology, Atlanta, GA 30332
Fax: 404-894-8336, E-mail: gtg506p@mail.gatech.edu

ABSTRACT

Electro-thermal, two-arm polysilicon actuators are widely employed in optical MEMS applications. These actuators are typically designed for maximum deflection (unloaded) or force (loaded) output characteristics. The optimal design methodology of the actuator has been investigated previously using trial and error analytical and semi-analytical methods. In this paper, design optimization of the electro-thermal actuator is attempted by a multi-variable non-linear comprehensive finite element analysis. The optimization subroutine is implemented to investigate and compare the performance of the actuator by adjusting the design variables to obtain an actuator geometry that provides optimum deflection or force output for minimal power consumption.

***Keywords*:** thermal actuators, finite element analysis, design optimization, ANSYS.

1 INTRODUCTION

MicroElectroMechanical Systems (MEMS) typically refer to devices having a length of less than 1 mm but greater than 1 μm, which combine electrical and mechanical components and are fabricated using Integrated Circuit (IC) technology. Microactuators, a critical component of most microsystems, precisely control the orientation and position of other MEMS components. The range of deflection and force provided by microactuators increase their functionality in microsystems. Many techniques for actuation have been established at the microscale. Out of these, electro-thermal actuation provides an easily controlled micro-actuation method compatible with standard microelectronics.

Guckel et al. [1] proposed a topology for an electro-thermally actuated microactuator, which has been developed extensively by Comtois and Bright [2-4]. This basic two-arm electro-thermal actuator design uses the principle of Joule heating for thermal expansion and movement. As shown in Fig.1, the two-arm actuator design consists of a thin arm, wide arm and flexure arm connected together at one end and constrained elastically at the anchors, which in turn are rigidly attached to the substrate. Application of a potential difference at the anchors generates a non-uniform electric field. The larger current density in the thin arm causes a greater thermal expansion than that in the wide arm, leading to motion of the actuator tip towards the wide arm. These actuators are typically fabricated by a MUMPs (Multi User MEMS Process) surface micromachining process that utilizes heavily doped polysilicon as the structural layer [5].

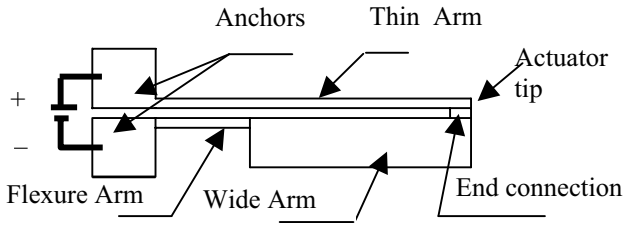

Figure 1. Basic two-arm electro-thermal actuator

This actuator has been employed extensively in optical MEMS applications for driving of optical mirrors and stepper motors mainly because of its simplicity in fabrication and ability to produce large deflections [2-4]. The main disadvantage of such electro-thermal actuators is the amount of power consumed to obtain the required deflection and force. Arrays of such actuators are coupled to increase the amount of delivered force, which again leads to increased drive power and space required. Improving the force and the deflection characteristics of an individual thermal actuator allows for fewer numbers of actuators to be employed in an array, decreasing the space requirements and power consumption.

In previous research on design of these devices for maximum deflection and force, Hickey [6] has laid down guidelines for optimization using a trial and error analytical approach. Chen et al. [7] have investigated the effect of dimensional variation on the actuator performance by analyzing various actuator designs using a semi-analytical approach.

In this paper, optimization of the electro-thermal actuator is attempted by a multi-variable non-linear comprehensive finite element analysis. The optimization subroutine is implemented to improve the deflection and force characteristics of the surface micromachined electro-thermal actuator at the same or lower power consumption levels. A generalized optimization batch file that includes temperature dependent material properties of heavily doped polysilicon, conduction to the silicon substrate through the

air gap, convection and radiation to the surroundings is developed, which can be utilized to completely analyze a specific actuator design or to study the effect of variation of design parameters on the performance of the electro-thermal actuator based on user specified limits [8]. The developed analysis provides a systematic method to design the two-arm electro-thermal actuator to meet various performance requirements.

2 ANALYSIS

The analysis of the actuator requires the solution of a generally nonlinearly coupled electro-thermal-elastic boundary value problem.

2.1 Boundary Conditions

Figure 2 shows a 3-D view of the actuator suspended above the substrate after release. The actuator arms are separated from the substrate by a 2 μm air gap, while the anchors remain attached to the substrate, which acts as a heat sink at an assumed ambient temperature [5]. A thin nitride layer separates the substrate from the air gap. The substrate, nitride layer, and the surrounding air are not modeled directly but their effects are included indirectly through various boundary conditions. An electrical potential difference V is applied across the anchors, which causes non-uniform Joule heating. The deflection of the actuator due to this heating is parallel to the substrate.

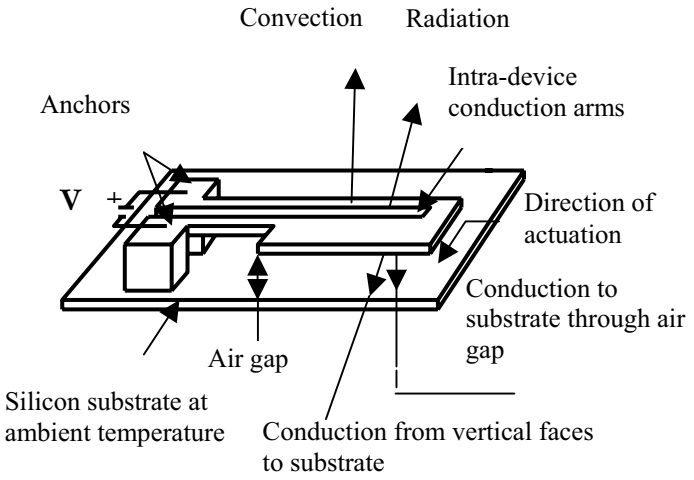

Figure 2. Boundary Conditions

Under normal modes of operation, the actuator will transfer heat to the surroundings and substrate by all three basic modes of heat transfer: conduction, convection and radiation, though some modes will dominate over the others.

The conductive heat loss to the substrate through the air gap is modeled as an effective conductive heat transfer coefficient defined as

$$h = \frac{1}{\left(t_a/k_a + t_n/k_n + t_{Si}/k_{Si}\right)} \quad (1)$$

A conductive shape factor S is used to account for the heat loss from the vertical faces to the substrate, expressed as [9]

$$S = \frac{t}{w}\left(\frac{2t_a}{t} + 1\right) + 1 \quad (2)$$

The convective heat loss from the top horizontal faces of the actuator is modeled by computing the heat transfer coefficients from the correlations developed for a heated horizontal face facing upwards [10]. Radiation is implemented directly in the finite element analysis. Table 1 lists the material property parameters used in the analysis. Each parameter shows its constant room temperature value and its temperature dependency if applicable. The thermal results from the electro-thermal analysis are applied as loads to obtain a quasi-static thermal-elastic solution. The boundary conditions for the structural problem are constraining the bottom faces of the anchors and applying the temperature field from the thermo-elastic analysis.

Parameter	Constant Value	Ref.
Elastic modulus of polysilicon	169 GPa	12
Poisson's ratio of polysilicon	0.22	12
Emmisivity	0.6	13
Stefan-Boltzmann constant	5.67×10^{-8} W-m^{-2}-^{o}C^{-4}	13
Thermal cond. of air (k_a)	0.026 W-m^{-1}- ^{o}C^{-1}	9
Thermal cond. of nitride (k_n)	2.25 W-m^{-1}- ^{o}C^{-1}	9
Thermal cond. of silicon (k_{Si})	150 W-m^{-1}-^{o}C^{-1}	14
Thermal conductivity of polysilicon (k_p)	32 W-m^{-1} -^{o}C^{-1}	13
Coeff. of thermal expansion of polysilicon (α)	2.7×10^{-6} K^{-1}	13
Electrical resistivity of polysilicon (ρ_0)	2×10^{-3} Ω-cm	15
Resistivity coefficient of polysilicon (α_r)	1.25×10^{-3} ^{o}C^{-1}	13
Temperature Dependencies		
$k_p(T)=[(-2.2*10^{-11})T^3 + (9.0*10^{-8})T^2 +(-1.0*10^{-5})T+0.014]^{-1}$ W-m^{-1}-^{o}C^{-1}		16
$\rho(T) =\rho_0[1+\alpha_r(T-T_0)]$		13
$\alpha_c(T)=(3.725\{1-\exp(-5.88*10^{-3}(T-125))\} +5.548*10^{-4}T)*10^{-6}$ K^{-1}		13
$k_a(T) = 3.9539 \times 10^{-4} + (9.886 \times 10^{-5})\,T - (4.367 \times 10^{-8})\,T^2 + (1.301 \times 10^{-11})\,T^3$ W-m^{-1}-^{o}K^{-1}		13

Table 1. Material property parameters

2.2 Simulation

The design optimization of the two-arm actuator is performed in ANSYS 6.1 finite element analysis simulation program using the coupled electro-thermal-elastic method for analysis [11]. Thermal radiation is modeled using the radiosity solver method available in ANSYS [11]. The design optimization command or batch file is created using the ANSYS Parametric Design Language (APDL) [11].

3 RESULTS

Table 2 compares the original and the optimized thermal actuator parameters. For an unloaded actuator the most significant difference in deflection is obtained from the increase in actuator length, decrease in the thin and wide arm spacing, an increase in the wide arm width and decrease in flexure length. This is consistent with experimental results.

The optimization subroutine determines the optimum flexure length for thermal actuator. It has been observed that as the applied voltage increases the optimum flexure length also increases. Table 2 shows the optimized actuator parameters for an applied voltage of 5 V. From the feasible design sets available the best thermal actuator that gives the maximum deflection for a lesser power consumption was selected as optimum.

This percentage reduction in power consumption and increase in maximum deflection is observed to remain consistent for the range of applied voltages. Figure 3 illustrates this point. The optimized thermal actuator shows a reduced maximum temperature for any applied voltage. This is mainly contributed by the change in the gap, the width of the wide arm and flexure arm length. The optimization comparison was done with the same applied voltage since this is the only input, which can be controlled and hence facilitates a comparison between the different actuator parameters. The optimization subroutine can also be employed to design a complete thermal actuator based on the changes in the design and state variable [8,11]. For example, specifying the applied voltage as a design variable within any required limits and the maximum temperature as a state variable allows for a complete selection of an optimized thermal actuator for the required maximum steady state deflection based on the design sets.

The optimization of loaded actuators requires significant optimization iterations for a complete design. This is because as the force provided by the thermal actuator increases the available deflection decreases. Since, the optimization subroutine is employed to minimize the deflection in this case, a tradeoff between the available force and deflection must be done. For an unloaded actuator the most significant difference in deflection is obtained from the increase in actuator length, decrease in the thin and wide arm spacing, an increase in the wide arm width and decrease in flexure length.

The optimization subroutine can be employed to design the thermal actuator based on a required steady-state deflection in order to optimize the force. Table 2 compares the original and optimized actuator parameters for loaded actuators. From the feasible design sets, the best thermal actuator that gave a higher force while giving a reasonable value of deflection for the same power consumed was chosen as the optimum.

Since the deflection is minimized the significant parameters that affect the force output from the thermal actuator are a decrease in the actuator length, increase in the width of the thin arm, decrease in the width of the wide arm and increase in the thin arm and wide arm spacing.

The flexure arm length in this case is observed to increase with the applied voltage. The typical optimized flexure arm length from the design sets is observed to be between 35-50 μm. The optimized thermal actuator shows an 8% increase in the force output from the original geometry for approximately the same power consumed. Further increase in the force output leads to a significant decrease in the deflection, which dominates over the benefit of obtaining more force. This trend remains consistent over the range of applied voltages (Figure 4).

4 CONCLUSIONS

This paper investigated the optimal design methodology of a two-arm surface micromachined horizontal electro-thermal actuator using finite element analysis. An indirect method was employed by maximizing the steady-state deflection for unloaded actuators and minimizing the steady-state deflection for loaded actuators for the same applied voltage. A generalized optimization batch file that includes all the relevant parameters was implemented in the analysis. A systematic process for optimal design of the electro-thermal actuator was also presented. The results reveal a significant reduction in power consumption with an increase in the maximum steady-state deflection for unloaded actuators. For loaded actuators the available force output is increased slightly, the steady-state deflection decreased slightly and the power consumption increased slightly.

REFERENCES

[1] Guckel, H., Klein, J., Christenson, T., Skrobis, K., Laudon, M., Lovell, E., "Thermo-magnetic metal flexure actuators," Technical digest, Solid State Sensor and Actuator Workshop, 1992, pp 73-75.

[2] Comtois, J .H., Bright Victor M., Phipps, M.W., "Thermal microactuators for surface-micromachining processes", *Proc. SPIE*, Vol.2642, 1995, pp. 10-21.

[3] Reid, J., Bright, V.M., Comtois, J., "Arrays of thermal microactuators coupled to micro-optical components," Actuator technology and Applications, vol. 2865, 1997, pp. 74-82.

[4] Comtois, J.H., Bright, V.M., "Applications for surface-micromachined polysilicon thermal actuators and arrays," *Sensors and Actuators A*, vol.58, 1997, pp.19-25.
[5] Koester, D., Mahadevan, R., Hardy, B., Markus, K., "Multi-user MEMs processes (MUMPs) Design Handbook," Cronos Integrated Microsystems, JDS Uniphase, NC, Revision 6.0, 2001.
[6] Hickey, R., "Analysis and Optimal Design of Micro-machined Thermal Actuators", M.A.Sc Thesis, Dalhousie University, Nova Scotia, CA, 2001.
[7] Chen, R.S., Kung, C., Lee, G., "Analysis of the optimal dimension on the electro thermal microactuator", *J.Micromech.Microeng.*, vol.12, pp. 291-296, 2002.
[8] Atre, A, "Steady State and Transient Analysis of Electro-Thermal Microactuators using Finite Element Methods", M.S. Thesis, Rochester Institute of Technology, Rochester, NY, 2003.
[9] Lin, L., Chiao, M., "Electrothermal responses of lineshape microstructures," *Sensors and Actuators A*, vol.55, 1996, pp.35-41.
[10] Mills, A., *Basic Heat and Mass Transfer*, 1999, Prentice Hall.
[11] ANSYS Online Help Manual, Version 6.1.
[12] Sharpe, W. N., Jr., Eby, M. A., and Coles, G., "Effect of Temperature on Mechanical Properties of Polysilicon," *Proc.Transducers'01*, pp 1366-1369, 2001.
[13] Lott, C.D., "Electrothermomechanical modeling of surface-micromachined linear displacement microactuator," M.S. Thesis, Brigham Young University, Provo, Utah, 2001.
[14] Mankame, N.D., "Modeling of electro-thermal-compliant mechanisms," M.S. Thesis, University of Pennsylvania, Philadelphia, PA, 2000.
[15] Cronos Integrated Microsystems, www.memsrus.com, JDS Uniphase.
[16] Manginell, R.P., "Polycrystalline- Silicon microbridge combustible gas sensor," Ph.D Thesis, University of New Mexico, Albuquerque, NM, 1997.

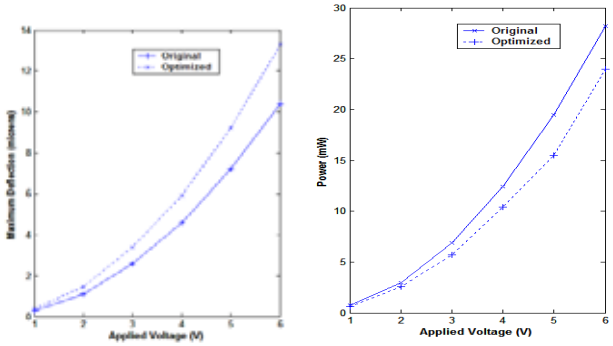

Figure 3. Comparison of original and optimized unloaded actuator performance for a range of applied voltages

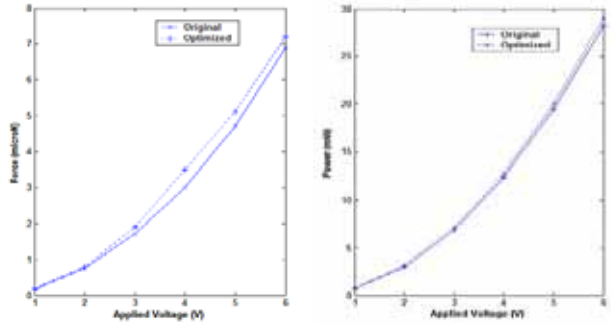

Figure 4. Comparison of original and optimized unloaded actuator performance for a range of applied voltages

Parameter	lt (μm)	lf (μm)	wt (μm)	ww (μm)	g (μm)	V	Max.Temp (C)	Deflection (μm)	Force (μN)	Current (mA)	Power (mW)
Inital	200	36	2	15	2	5	673	7.2	4.7	3.9	19.9
Optimized-Unloaded	200	30	2	16	1.75	5	510	9.2	na	3.1	15.5
Optimized-Loaded	235	50	2.8	13	3	5	543	5.2	5.1	4	20

Table 2. Comparison of original and optimized actuator parameters for maximum steady-state deflection and maximum force output. (l_t – length of thin arm, l_f – length of flexure arm, w_t – width of thin arm, w_w – width of wide arm, g – arm spacing, V-applied voltage)